



SIMULATION OF DYNAMIC RESPONSE OF SATURATED SANDS USING MODIFIED DSC MODEL

Soo-il KIM¹, Jae-soon CHOI², Keun-bo PARK³, Kyung-bum SEO⁴, Jun-hwan LEE⁵

SUMMARY

A modified disturbed state concept (DSC) model to simulate the dynamic behavior of saturated sands was proposed in this paper. Laboratory dynamic tests were performed to verify the modified DSC model. Based on the test results, it is concluded that the modified DSC model simulates reasonably well dynamic responses of saturated sands including excess pore water pressure, stress degradation, initial liquefaction occurrence, and post-liquefaction behavior. A numerical back-predict program based on the incremental solution of the modified DSC model was also developed.

INTRODUCTION

Excess pore water pressure is an important consideration for a seismic design. Several models were developed to describe dynamic responses of saturated sands. Those included Finn [1], Desai [2], and Iai [3] models. According to Finn [1], it is assumed that the excess pore water pressure with cyclic loading is related to the volumetric strain in a drained condition. For modeling the liquefaction behavior, Iai [3] introduced the phase transformation line and liquefaction front associated with the accumulative process of shear work. The disturbed state concept (DSC) was first introduced by Desai [4] to characterize the stress softening behavior of overconsolidated soils. In the DSC model, observed or average response of geological materials is expressed by the two reference states. One is the relative intact (RI) state that is defined using continuum models such as elastic and plastic models, and the other is the fully adjusted (FA) state that represents responses of materials at failure. The DSC model has been successfully verified in various dynamic problems, but it has several limitations. The DSC model requires large number of parameters to define two reference states, the RI and FA states. In addition, the DSC model cannot explain the rapid degradation of the mean effective stress observed at an initial liquefaction stage and a failure mode at the ultimate state. In order to overcome those limitations, the modified DSC model was developed. Laboratory static and cyclic triaxial tests were performed and compared with back-predicted results using the modified DSC model.

¹ Professor, Yonsei University, Seoul, Korea. Email: geotech@yonsei.ac.kr

² Postdoctoral Associate, Yonsei University, Seoul, Korea. Email: geocjs@yonsei.ac.kr

³ Ph. D. Student, Yonsei University, Seoul, Korea. Email: uscake@yonsei.ac.kr

⁴ Ph. D. Student, Yonsei University, Seoul, Korea. Email: kbseo@yonsei.ac.kr

⁵ Assistant Professor, Yonsei University, Seoul, Korea. Email: junlee@yonsei.ac.kr

THE DSC AND MODIFIED DSC MODELS

DSC MODEL

The DSC model is based on the idea that a mixture's response can be expressed in terms of the responses of its interacting components. The components are considered to be material parts in the RI or continuum state and in the FA state. As loading progresses, the material transforms progressively from the RI state to the FA state through a process of self-adjustment as shown in Fig. 1. Applied forces cause disturbance or change in the microstructure of a material. Consequently, the observed or average response can be represented in terms of responses of materials in the two reference states, the RI and FA states (Desai, [5]).

In the DSC model, the RI state is characterized by Hierarchical Single Surface (HiSS) model with the isotropic hardening and associated flow rule as shown in Fig. 2 (Desai [6]). The FA state implies a state in which the material under a given initial hydrostatic stress continues to deform in shear with a constant volume as in the critical state concept.

The disturbance and the observed effective stress in the DSC model can be expressed as follows:

$$D = \frac{\bar{\sigma}_{ij}^i - \bar{\sigma}_{ij}^a}{\bar{\sigma}_{ij}^i - \bar{\sigma}_{ij}^c} \quad (1)$$

$$\bar{\sigma}_{ij}^a = (1-D)\bar{\sigma}_{ij}^i + D\bar{\sigma}_{ij}^c \quad (2)$$

where D = disturbance; $\bar{\sigma}_{ij}^a$, $\bar{\sigma}_{ij}^i$, and $\bar{\sigma}_{ij}^c$ = effective stresses in the observed, relative intact, and fully adjusted states in Fig. 1, respectively. According to Armaleh [7], the disturbance function for a relationship between D and ξ_D is defined as follows:

$$D = D_u \left[1 - \exp\left(-A \xi_D^Z\right) \right] \quad (3)$$

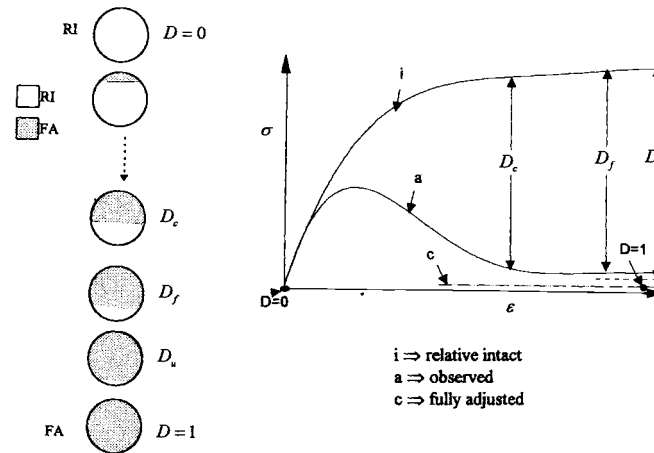


Fig. 1. Representation of DSC (Desai [8]).

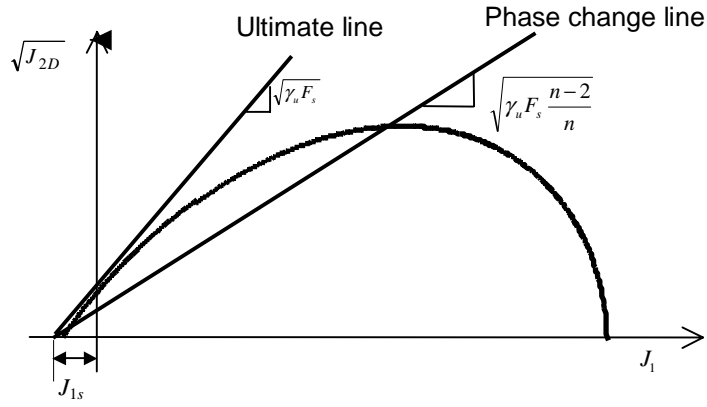


Fig. 2. Yield surface, phase change line, and ultimate line in HiSS model (Desai [6]).

where A , Z , and D_u are material parameters. The deviatoric plastic strain trajectory ξ_D in (3) is given by:

$$\xi_D = \int \sqrt{dE_{ij}^p dE_{ij}^p} \quad (4)$$

The deviatoric plastic strain trajectory is calculated by the summation of deviatoric plastic strains as shown in Fig. 3. In Fig. 3, deviatoric plastic strain trajectories are assumed to be equal to the summation of shear works calculated by the area of hysteric loops. Fig. 4 shows a typical shape of the disturbance function curve in terms of disturbances and deviatoric plastic strain trajectories. The incremental constitutive equation for the DSC model can be obtained by differentiating (4) as follows (Desai [8]):

$$d\sigma_{ij}^a = (1-D)d\sigma_{ij}^i + Dd\sigma_{ij}^c + dD(\sigma_{ij}^c - \sigma_{ij}^i) \quad (5)$$

where superscripts a , i , and c denote the observed, relative intact, and critical states, respectively.

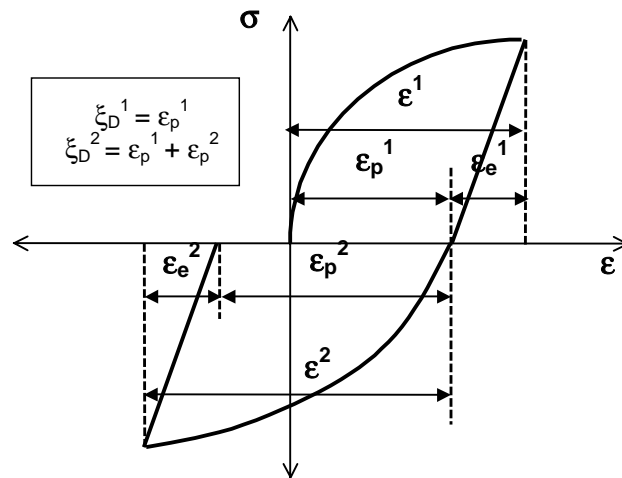


Fig. 3. Determination of the deviatoric plastic strain trajectory.

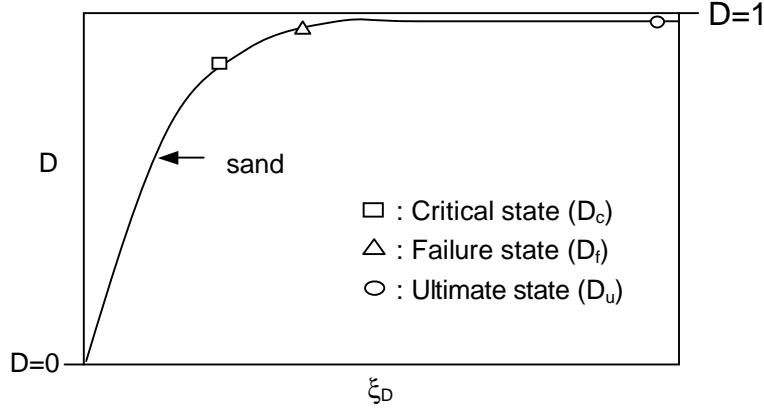


Fig. 4. Disturbance function curves between D and ξ_D (Desai [8]; Kim [9]).

MODIFIED DSC MODEL

Through our research, it is found that there are several disadvantages in the original DSC model. Fig. 5 shows an effective stress path of fully saturated sands under cyclic loadings. From Fig. 5, it can be seen that the dynamic behavior of soils can be divided into three parts: gradual degradation of effective mean stress, rapid degradation until an initial liquefaction occurrence, and failure behaviors after an initial liquefaction (i.e. post-liquefaction behavior). However, the original DSC model does not consider the rapid degradation of the mean effective stress for an initial liquefaction and the ultimate failure mode after initial liquefaction. The original DSC model also requires a large number of parameters associated with the RI state and the FA state. For which, more than three static tests and a dynamic test should be performed for parameter determination.

In order to overcome such disadvantages, the original DSC model was modified. In the modified DSC model, the RI state is defined using HiSS model as in the original DSC model, whereas the FA state is defined using the Drucker-Prager model [10]. Under the condition of isotropic hardening, a single yield surface function F in $J_1 - \sqrt{J_{2D}}$ space in HiSS model proposed by Desai [6] is given by:

$$F = \frac{J_{2D}}{p_a^2} - \left[-\alpha \left(\frac{J_1 + J_{1s}}{p_a} \right)^n + \gamma_u \left(\frac{J_1 + J_{1s}}{p_a} \right)^2 \right] \quad (6)$$

where p_a is the atmospheric pressure as the same unit as a stress and J_{1s} is the shift of J_1 axis resulting from the tensile strength of material. In general, p_a is 101.3 kPa and J_{1s} of fully saturated sands is almost zero. In (6), soil parameters n and γ_u are determined from static tests. A hardening function α plays an important role in defining the work hardening behavior. The hardening function α proposed by Rigby and Desai [11] is given as:

$$\alpha = \frac{h_1}{\xi_D^{h_2}} \quad (7)$$

where h_1 and h_2 are material plastic parameters.

For the ultimate state under incremental static loading conditions, it is known that the maximum deviatoric stress is over 1 MPa, which is hardly achieved in conventional laboratory tests. On the other hand, the dynamic test result shows the ultimate state behaviors clearly after an initial liquefaction as

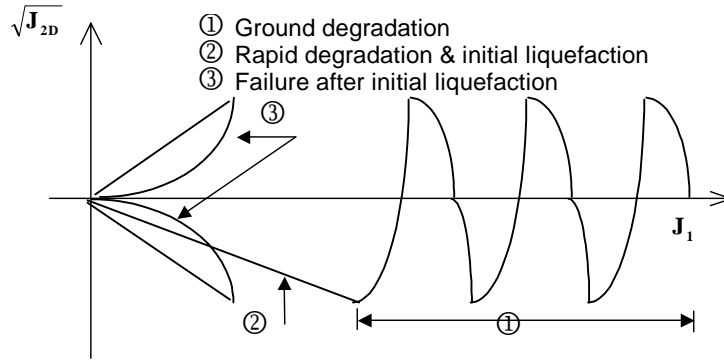


Fig. 5. Effective stress path of fully saturated sands under cyclic loadings (Kim [9]).

shown in Fig. 5. Based on this observation, the FA state in the modified DSC model is defined at post liquefaction state of the dynamic test result. It is also assumed that the slope of effective stress path after initial liquefaction is the same as the slope of the ultimate line in Fig. 2. From these assumptions, the slope m of failure criterion for the Drucker-Prager model is equal to $\sqrt{\gamma_u}$ for the ultimate line of HiSS model.

Parameters used in the original and modified DSC models are summarized in Table 1. In the Table 1, it is seen that the number of parameters required for the modified DSC model is smaller than that for the original DSC model. In the modified DSC model, the three FA parameters of the original DSC model based on the critical state concept need not to be determined separately because the only FA parameter m can be obtained from the RI parameter γ_u . Modifying the two reference states, most terms in (5) are changed from those of the original DSC model.

Table 1. Summary of DSC parameters.

Material state	Group	DSC parameters	
		Original	Modified
Relative intact (RI) state	Elastic parameters	E	E
		ν	ν
	Plastic parameters	γ_u	$\gamma_u (= m^2)$
		$\beta = 0$	$\beta = 0$
		n	n
		h_1	h_1
Fully adjusted (FA) state	Ultimate state parameters	\bar{m}	m
		λ	$k (= 0)$
		e_o^c	-
Observed state	Disturbance function parameters	$D_u = 0.99$	$D_u = 0.99$
		Z	Z
		A	A

LABORATORY TESTS AND PARAMETER DETERMINATION

In order to verify the modified DSC model, cyclic and static triaxial tests were performed. Soils used in the tests were Jumunjin sand, representative silica sand in Korea. Properties of the soil are given in Table 2. In the tests, soil samples were saturated until the value of a pore water pressure parameter B is at lowest 0.97. Additional cell pressure is then applied allowing consolidation for one hour. In this study, two different confining pressures equal to 100 and 150 kPa were used. For cyclic triaxial tests, cyclic loadings were applied at a frequency of 0.1 Hz. Test results for static and cyclic loading conditions with a stress ratio of 0.22 are shown in Figs. 6 through 8.

Table 2. Properties of Jumunjin sand.

Max. unit weight γ_{\max} (kg/cm ³)	Min. unit weight γ_{\min} (kg/cm ³)	Mean grain size D ₅₀ (mm)	Coeff. of uniformity, C _u	Coeff. of curvature, C _c
1.60	1.39	0.52	1.35	1.14

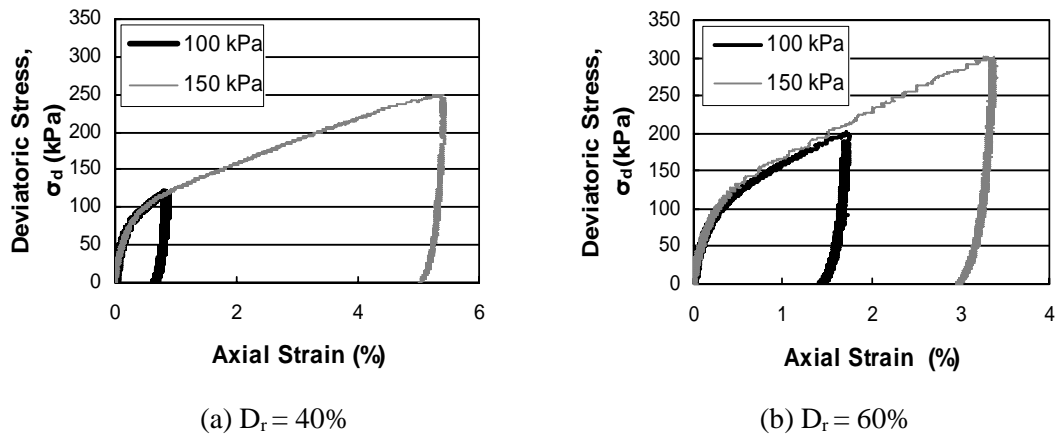


Fig. 6. Stress-strain behavior from static triaxial tests.

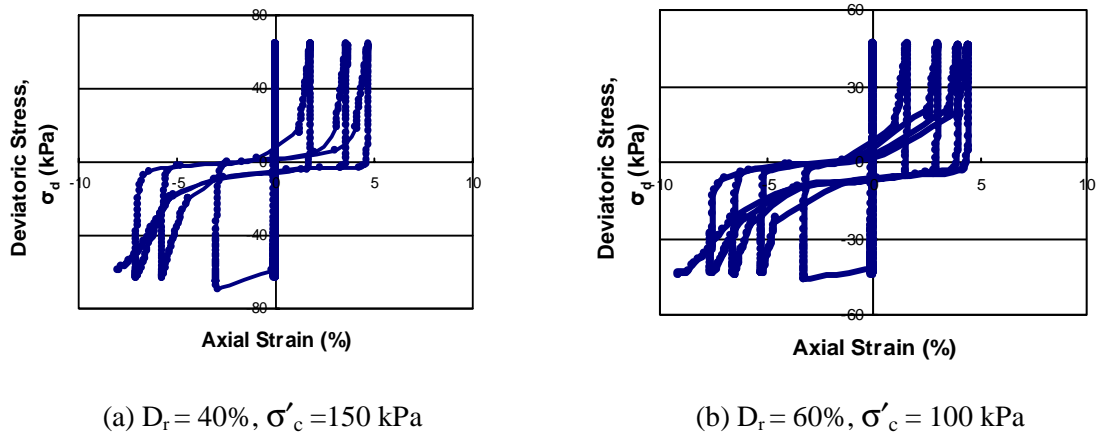
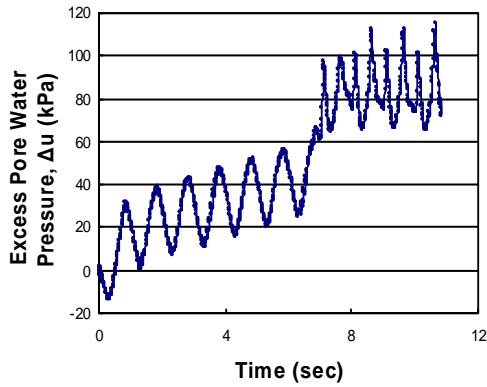
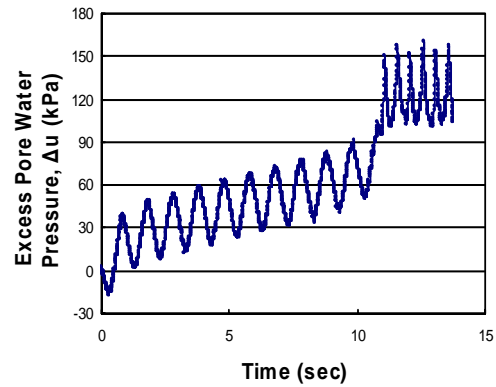


Fig. 7. Stress-strain behavior from cyclic triaxial tests.



(a) $D_r = 40\%$, $\sigma'_c = 150$ kPa



(b) $D_r = 60\%$, $\sigma'_c = 100$ kPa

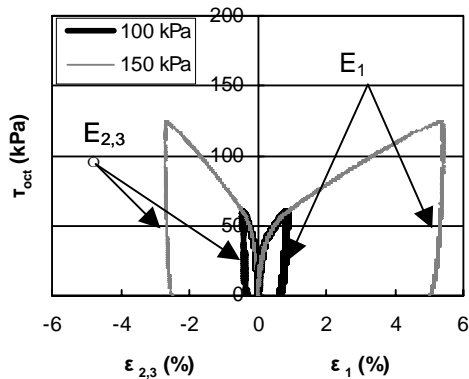
Fig. 8. Mobilization of excess pore water pressure in cyclic triaxial tests.

Parameters used in the modified DSC model can be grouped into three categories, according to material states, as listed in the Table 1. Determination of parameters for different material states is described in following section.

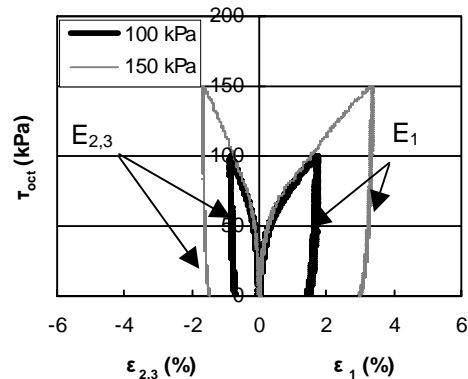
Material parameters for RI state

Elastic parameters

For an isotropic linear elastic material, description of the stress-strain behavior requires two elastic constants, Young's modulus E and Poisson's ratio ν . Poisson's ratio ν was obtained from strains when a soil sample is consolidated under hydrostatic compression loadings. Poisson's ratio ν from the test results was determined to be 0.38. Young's modulus E can be evaluated from static triaxial compression (TC) tests. Fig. 9 shows slopes E_i , (where $i = 1, 2,$ and 3 represents the three principal directions), which corresponds to the slope of unloading curves in TC tests. After measuring these slopes E_i , elastic constants E were evaluated from equations given in Table 3. Values of E were found to be 175000 and 210000 kPa for $D_r = 40\%$ with $\sigma'_c = 150$ kPa and $D_r = 60\%$ with $\sigma'_c = 100$ kPa, respectively.



(a) $D_r = 40\%$



(b) $D_r = 60\%$

Fig. 9. $\tau_{oct} - \epsilon_i$ relationship from static triaxial tests.

Table 3. Relations between elastic constants (Desai [5]).

Stress path	E	ν
CTC RTE	$\frac{3}{\sqrt{2}}E_1$	$\frac{2 E_1 }{ E_2 + E_3 }$
CTE RTC	$\frac{3\sqrt{2} E_1 (E_2 + E_3)}{4 E_1 + E_2 + E_3 }$	$\frac{ E_2 + E_3 }{4 E_1 }$
TC TE	$\frac{\sqrt{2}}{3}(1+\nu)(E_1 + E_2 + E_3)$	-
SS	$\frac{\sqrt{2}}{3}(1+\nu)(E_1 + E_3)$	-

$$E_i = \text{slope on } \tau_{oct} \text{ vs. } \varepsilon_i \text{ plot}$$

$$\tau_{oct} = \frac{\sqrt{(\sigma_1 - \sigma_3)^2 + (\sigma_2 - \sigma_3)^2 + (\sigma_1 - \sigma_2)^2}}{3}$$

Plastic parameters

The phase change parameter n , shown in Fig. 2, can be determined from static compression tests as in the original DSC model. The ultimate parameter γ_u can also be determined from the same experimental results. The ultimate state is difficult to capture clearly as the deformation develops continuously in the static shear test. It is, however, easy to capture the ultimate state after initial liquefaction in the dynamic laboratory test.

Figs. 10 and 11 show the phase change lines from static tests and stress paths from cyclic tests, respectively. From Fig. 11, it is seen that the rapid stress degradation starts when the effective stress path meets the phase change line determined from the static test. Fig. 11 also shows the ultimate lines obtained from cyclic tests. Based on the definition of the phase change line and the ultimate line shown in Fig. 2, values of n and γ_u of Jumunjin sand were found to be 2.795 and 0.203 for $D_r = 40\%$, and 2.667 and 0.250 for $D_r = 60\%$, respectively.

For the determination of plastic parameters h_1 and h_2 associated with the hardening function, values of α are calculated using $F = 0$ at every stress points as follows:

$$\alpha = \frac{\gamma_u \left(\frac{J_1}{p_a} \right)^2 - \left(\frac{\sqrt{J_{2D}}}{p_a} \right)^2}{\left(\frac{J_1}{p_a} \right)^n} \quad (8)$$

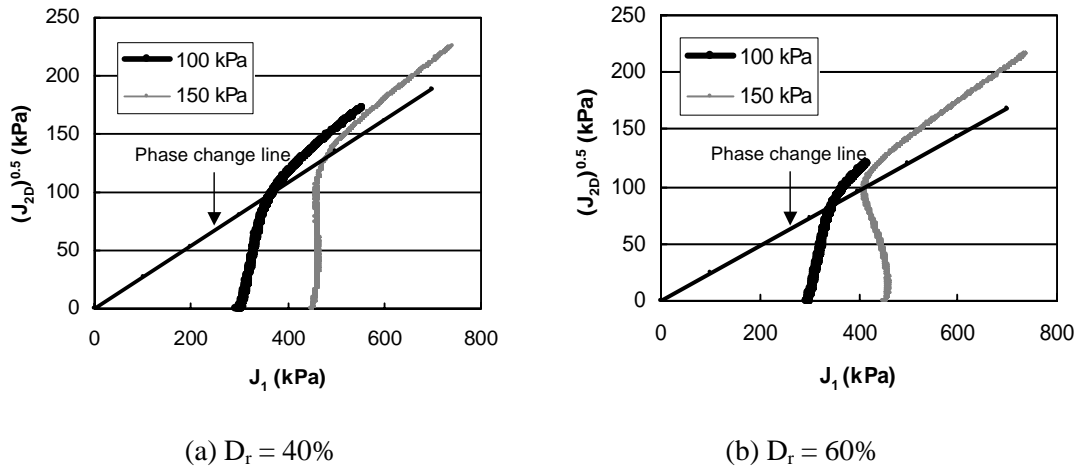


Fig. 10. Determination of phase change line from static triaxial tests.

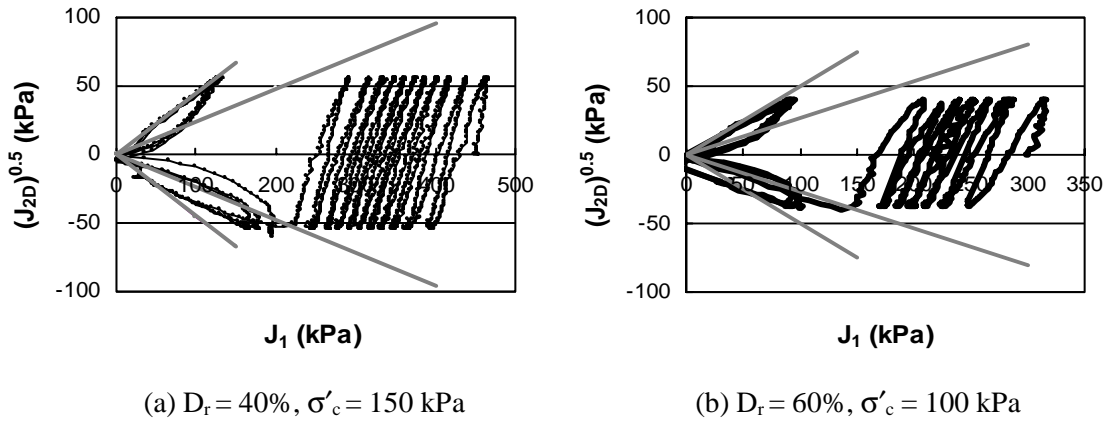


Fig. 11. Stress paths and ultimate lines from cyclic tests.

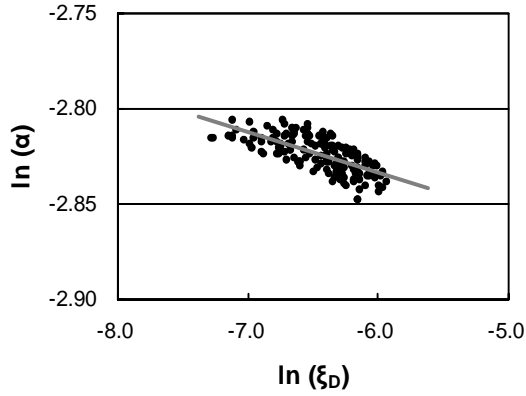
The trajectory of deviatoric plastic strain ξ_D is calculated using (4) by subtracting elastic strain from total strain at the same stress point. From a relationship between α and ξ_D , as shown in Fig. 12, one can determine the best fitting line to evaluate h_1 and h_2 using (7). From Fig. 12, values of h_1 and h_2 for Jumunjin sand were determined as 0.0588 and 0.0163 for $D_r = 40\%$ with $\sigma'_c = 150$ kPa, and 0.1515 and 0.0922 for $D_r = 60\%$ with $\sigma'_c = 100$ kPa, respectively.

Material parameters for FA state

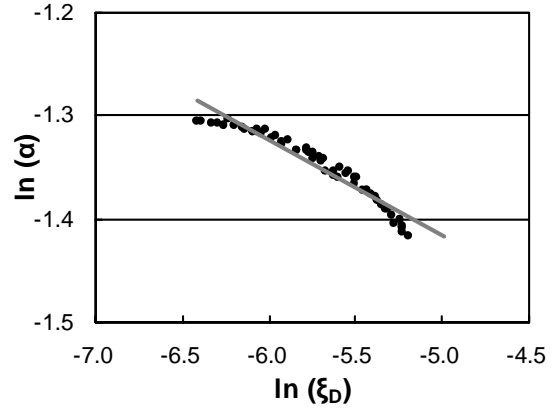
In the modified DSC model, FA state parameters m and k related to the ultimate failure line are determined from the Drucker-Prager model. Value of m is same as the value of $\sqrt{\gamma_u}$ and value of k is close to zero.

Material parameters for observed state

The observed state is expressed by the disturbance function as given by (3). While the parameter D_u can be assumed to be constant (Armaleh [7]), the disturbance D and the deviatoric plastic strain trajectory ξ_D are calculated from cyclic test results. In this study, D and ξ_D were calculated using (4) and (9) at every



(a) $D_r = 40\%$, $\sigma'_c = 150$ kPa



(b) $D_r = 60\%$, $\sigma'_c = 100$ kPa

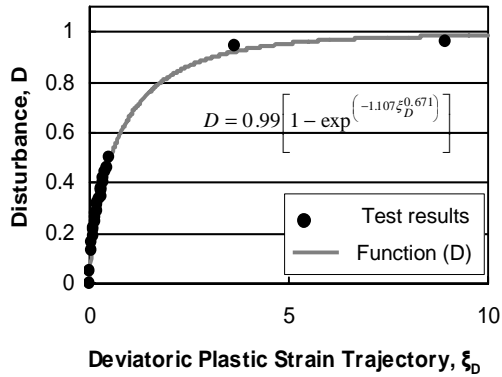
Fig. 12. Relationship between α and ξ_D .

fourth cycle from cyclic triaxial tests.

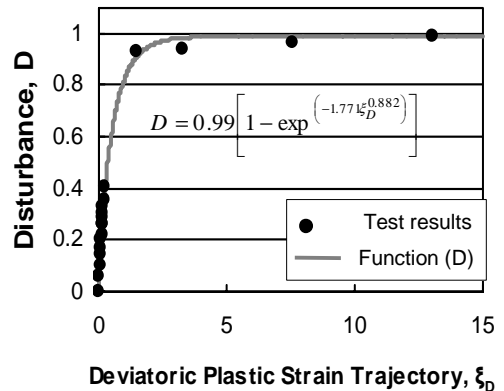
$$D = \frac{J_1^i - J_1^a}{J_1^i - J_1^c} \quad (9)$$

where J_1^i , J_1^a , and J_1^c = the first-order stress invariant at relative intact, observed, and critical states, respectively.

Disturbance function parameters A and Z in (3) were determined using the best fitting curves for the relationship between D and ξ_D . Solid lines in Fig. 13 show the fitting curves for the relationship between D and ξ_D using parameters A and Z . Fig. 14 shows values of disturbance D obtained from (9) and pore water pressure ratios $\Delta u/\sigma'_c$ obtained from the cyclic triaxial tests according to the number of cycles. As shown in Fig. 14, excellent matches between D and $\Delta u/\sigma'_c$ are observed. Results in Figs. 13 and 14 indicate that the disturbance D can be used as an index for the assessment of liquefaction potential.

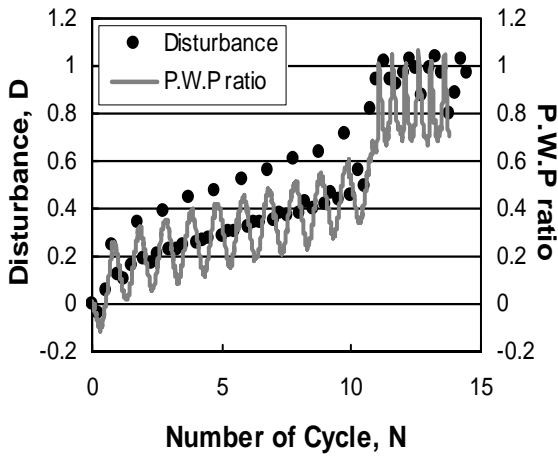


(a) $D_r = 40\%$, $\sigma'_c = 150$ kPa

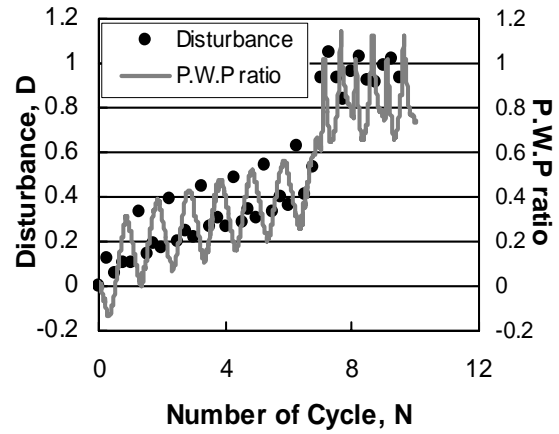


(b) $D_r = 60\%$, $\sigma'_c = 100$ kPa

Fig. 13. Relationships between D and ξ_D .



(a) $D_r = 40\%$, $\sigma'_c = 150$ kPa



(b) $D_r = 60\%$, $\sigma'_c = 100$ kPa

Fig. 14. Values of D and $\Delta u / \sigma'_c$ with number of loading cycles.

VERIFICATION OF THE MODIFIED DSC MODEL

A back prediction program based on the incremental integration scheme was developed to verify the modified DSC model. Through the procedure of parameter determination described previously, input DSC parameters were obtained and summarized in Table 4. In the program, the modified DSC model is used for representing compression and extension behaviors whereas the linear elastic model is used for unloading behavior. A detailed algorithm of the program is shown in Fig. 15.

Table 4. Input parameters used in back prediction.

Parameters	$D_r = 40\%$	$D_r = 60\%$
E	175000 kPa	210000 kPa
ν	0.38	0.38
γ_u	0.203	0.250
β	0	0
n	2.795	2.667
h_1	0.0588	0.1515
h_2	0.0163	0.0922
m	0.45	0.5
k	0	0
D_u	0.99	0.99
A	1.107	1.771
Z	0.671	0.882

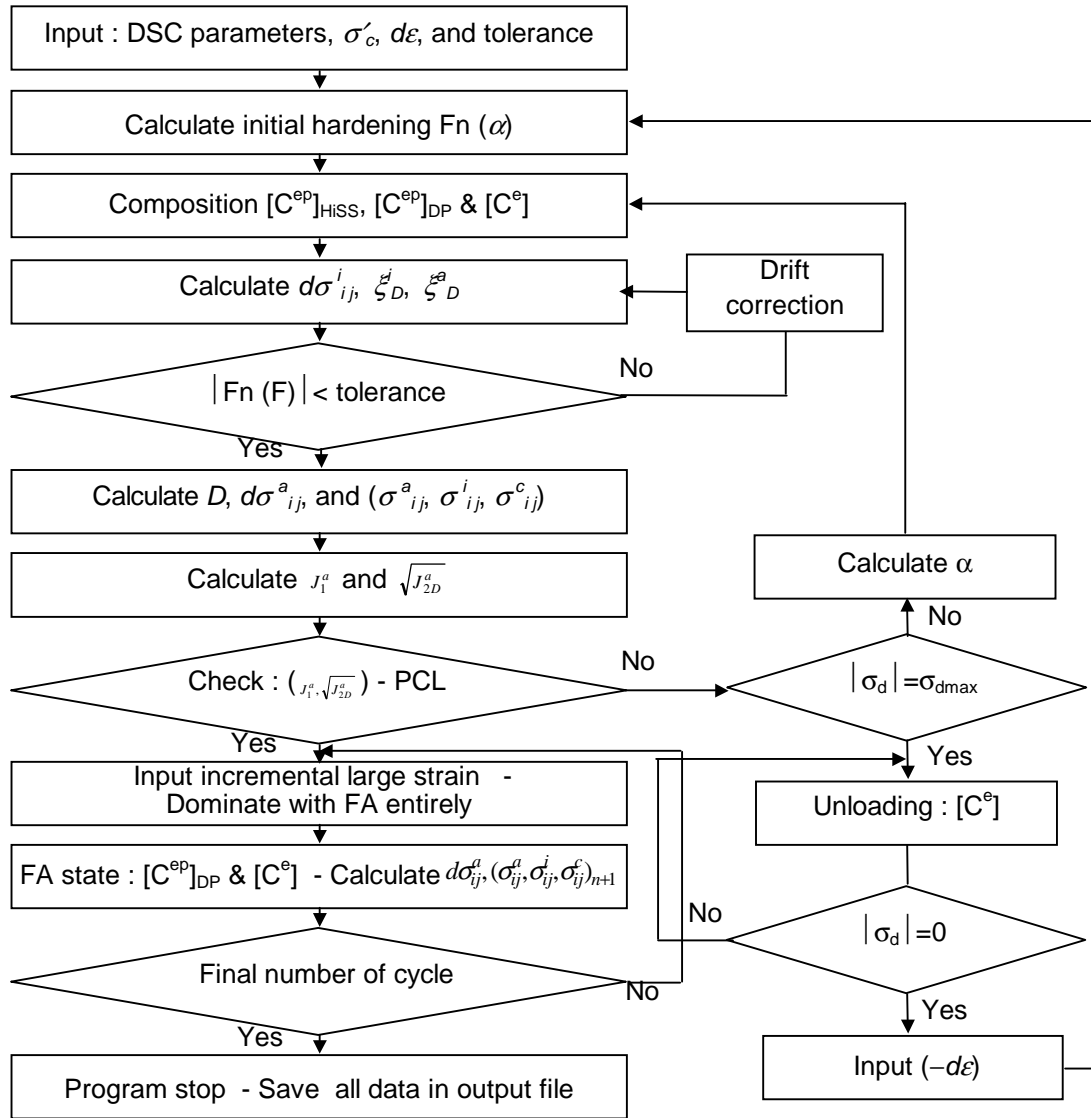
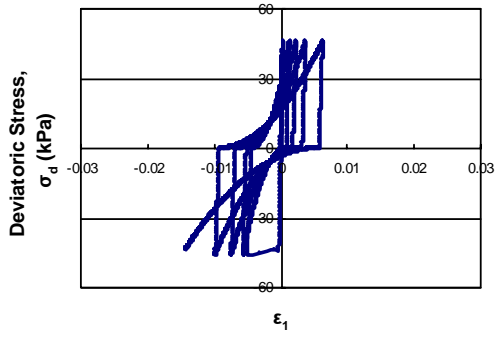


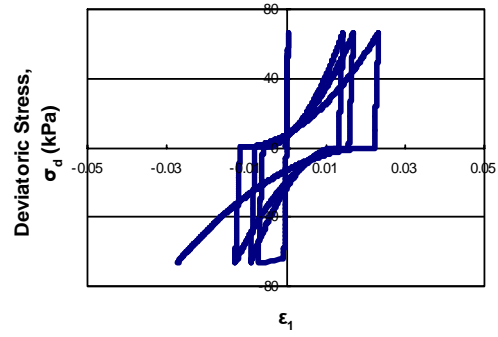
Fig. 15. Computation procedure of back prediction program using the modified DSC model.

Figs. 16 through 18 show results of back prediction. Compared with experimental results in Figs. 8 and 11, it is seen that back-predicted pore pressures and stress paths match well with the observed results. In particular, a better match is found in the harmonic behavior of the rapid stress degradation and initial liquefaction occurrence in stress paths. On the other hand, it is found that back-predicted stress-strain behaviors in Fig. 16 do not well reproduce observed results of Fig. 7. This is because soils behave as a composite liquid in the range of large deformation. A further investigation associated with the large deformation conditions would be necessary to define the post-liquefaction behavior.

Based on the result of back predictions, it can be concluded that the modified DSC model is effective for the analysis of the dynamic behavior of saturated sands and prediction of an initial liquefaction, while it produces stiffer stress-strain behavior than observed results after an initial liquefaction.

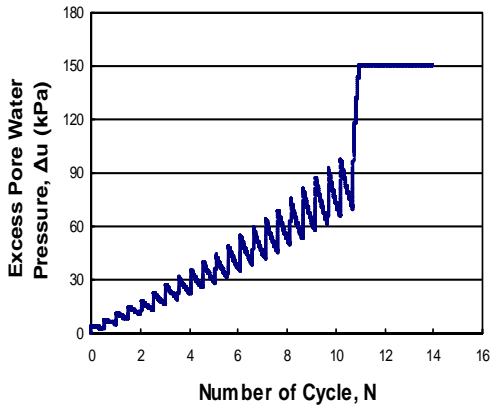


(a) $D_r = 40\%$, $\sigma'_c = 150$ kPa

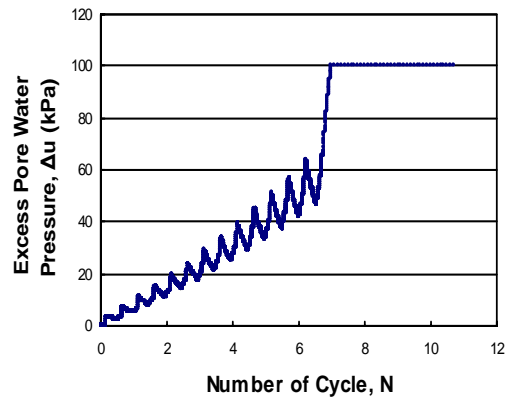


(b) $D_r = 60\%$, $\sigma'_c = 100$ kPa

Fig. 16. Results of back prediction (stress-strain relationship).

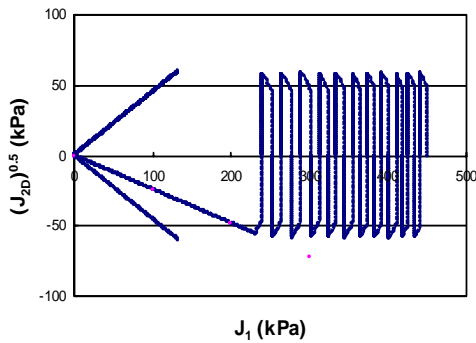


(a) $D_r = 40\%$, $\sigma'_c = 150$ kPa

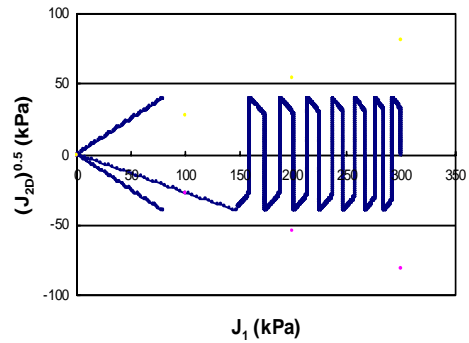


(b) $D_r = 60\%$, $\sigma'_c = 100$ kPa

Fig. 17. Results of back prediction (excess pore water pressure).



(a) $D_r = 40\%$, $\sigma'_c = 150$ kPa



(b) $D_r = 60\%$, $\sigma'_c = 100$ kPa

Fig. 18. Results of back prediction (stress path).

CONCLUSIONS

In this paper, the DSC model was investigated and modified for better simulation of the dynamic response of saturated sandy soils. Compared with original DSC model, the modified DSC model has some advantages. The modified DSC model requires smaller number of parameters than the original DSC model while it explains well a rapid degradation of effective mean pressure and a failure mode in the ultimate state. In order to verify the modified DSC model, a numerical program based on the incremental solution of integral scheme was developed and used for the back prediction of experimental results. Back-predicted results showed good agreements with the observed results at the initial liquefaction at which saturated sands behave as a mixing liquid. Based on the back-predicted results, it is concluded that the modified DSC model is effective for the description of mobilized excess pore water pressure and effective stress path under dynamic conditions.

REFERENCES

1. Finn, W. D. L., Lee, K. W. & Martin, G. R. 1977. "An effective stress model for liquefaction." *J. Geotech. Engrg. Div., ASCE*, Vol. 103, No. GT6: 517-533.
2. Desai, C. S. & Galagoda, H. M. 1989. "Earthquake analysis with generalized plasticity model for saturated soils." *J. Earthquake Engrg. and Struct. Dyn.* 18(6): 903-919.
3. Iai, S., Matsunaga, Y. & Kameoka, T. 1992. "Strain space plasticity model for cyclic mobility." *Int. J. Japanese Society of Soil Mech. and Found. Engrg.* 32(2): 1-15.
4. Desai, C. S. 1980. "A general basis for yield, failure and potential functions in plasticity." *Int. J. Numer. Analytical Methods in Geomech.* 4: 361-375.
5. Desai, C. S. 2001. "Mechanics of materials and interfaces." CRC Press, New York.
6. Desai, C. S., Sharma, K. G., Wathugala, G. W. & Rigby, D. B. 1991. "Implementation of hierarchical single surface δ_0 and δ_1 models in finite element procedure." *Int. J. Numer. Analytical Methods in Geomech.* 15: 649-680.
7. Armaleh, A. S. & Desai, C. S. 1990. "Modeling including testing of cohesionless soils under distributed state concept." Rep. to the Nat. Science Found., Department of Civil Engineering and Engineering Mechanics, Univ. of Arizona, Tucson, Arizona.
8. Desai, C. S., Park, I. J. & Shao, C. 1998. "Fundamental yet simplified model for liquefaction instability." *Int. J. Numer. Analytical Methods in Geomech.* 22(7): 721-748.
9. Kim, S. I. & Choi, J. S. 2003. "Application of disturbed state concept for the dynamic behaviors of fully saturated soils." *Proc., EESK Conf. Spring 2003*, 7(1): 140-147.
10. Drucker, D. C. & Prager, W. 1952. "Soil mechanics and plastic analysis or limit design." *The Quarterly J. Mech. and Applied Math.* 10(2): 157-165.
11. Rigby, D. B. & Desai, C. S. 1996. "Modeling of interface behavior using the cyclic multi-degree-of-freedom shear device with pore water pressures." Rep. to NSF, Dept. of Civil Engrg. and Mech., Univ. of Arizona, Tucson, Arizona.